THE EUROPEAN
PHYSICAL JOURNAL C

CrossMark

The sensitivity of the ICAL detector at India-based Neutrino Observatory to neutrino oscillation parameters

Daljeet Kaur[a], **Md. Naimuddin**[b], **Sanjeev Kumar**[c]

Department of Physics and Astrophysics, University of Delhi, Delhi 110007, India

Abstract The India-based Neutrino Observatory will host a 50 kt magnetized iron calorimeter (ICAL) detector that will be able to detect muon tracks and hadron showers produced by charged-current muon neutrino interactions in the detector. The ICAL experiment will be able to determine the precision of atmospheric neutrino mixing parameters and neutrino mass hierarchy using atmospheric muon neutrinos through the earth matter effect. In this paper, we report on the sensitivity for the atmospheric neutrino mixing parameters ($\sin^2 \theta_{23}$ and $|\Delta m^2_{32}|$) and octant sensitivity for the ICAL detector using the reconstructed neutrino energy and muon direction as observables. We apply realistic resolutions and efficiencies obtained by the ICAL collaboration with a GEANT4-based simulation to reconstruct neutrino energy and muon direction. Our study shows that using neutrino energy and muon direction as observables for a χ^2 analysis, the ICAL detector can measure $\sin^2 \theta_{23}$ and $|\Delta m^2_{32}|$ with 13 % and 4 % uncertainties at 1σ confidence level and can rule out the wrong octant of θ_{23} with 2σ confidence level for 10 years of exposure.

1 Introduction

Accumulation of more and stronger evidences of neutrino oscillations from several outstanding neutrino oscillation experiments with atmospheric [1–5], solar [6–16] and reactor [17–20] neutrinos have proven beyond any doubt that neutrinos have mass and they oscillate. In fact, neutrino oscillations were the first unambiguous hint for physics beyond the standard model of elementary particles. In the standard framework of oscillations, the neutrino flavor states are linear superpositions of the mass eigenstates with well defined masses:

[a] e-mail: daljeet.kaur97@gmail.com

[b] e-mail: nayeemsworld@gmail.com

[c] e-mail: sanjeev3kumar@gmail.com

$$|\nu_\alpha\rangle = \sum_i U_{\alpha i} |\nu_i\rangle , \tag{1}$$

where U is the 3×3 unitary Pontecorvo–Maki–Nakagawa–Sakata (PMNS) [21,22] mixing matrix. In the standard parameterisation [23], the PMNS matrix is given as:

$$U^{PMNS} = \begin{pmatrix} c_{12}c_{13} & s_{12}c_{13} & s_{13}e^{-i\delta} \\ -s_{12}c_{23} - c_{12}s_{23}s_{13}e^{i\delta} & c_{12}c_{23} - s_{12}s_{23}s_{13}e^{i\delta} & s_{23}c_{13} \\ s_{12}s_{23} - c_{12}c_{23}s_{13}e^{i\delta} & -c_{12}s_{23} - s_{12}c_{23}s_{13}e^{i\delta} & c_{23}c_{13} \end{pmatrix}. \tag{2}$$

Here, $c_{ij} = \cos \theta_{ij}$, $s_{ij} = \sin \theta_{ij}$ and δ is the charge-parity (CP) violating phase. The neutrino mixing matrix U^{PMNS} can be parameterized in terms of three mixing angles θ_{12}, θ_{23} and θ_{13}, and a CP phase δ so that neutrino oscillations are determined in terms of these parameters as well as two mass squared differences, Δm^2_{21} and Δm^2_{32}. The neutrino oscillations are only sensitive to differences of the squares of three neutrino masses m_1, m_2 and m_3: $\Delta m^2_{21} = m^2_2 - m^2_1$ and $\Delta m^2_{32} = m^2_3 - m^2_2$.

The parameters Δm^2_{21} and θ_{12} are constrained by the solar neutrino experiments. The atmospheric oscillation parameters Δm^2_{32} and θ_{23} were first constrained by the Super-Kamiokande [1] experiment. The sensitivities of these atmospheric parameters were further improved by the MINOS [3] and T2K [4] experiments. Recently, the DAYA Bay [19], RENO [20], MINOS [24] and T2K [25] experiments have measured the third mixing angle θ_{13}. With the conclusive measurement of relatively large and non-zero value of θ_{13} from these experiments, the effect of CP violation in neutrino oscillations is expected to be within the reach of future neutrino experiments. This discovery has also opened up a possibility to answer the various unsolved issues of current neutrino physics like whether the neutrino mass hierarchy is normal ($m^2_3 > m^2_2$) or inverted ($m^2_3 < m^2_2$), what the octant of θ_{23} is (whether $\theta_{23} < 45°$ or $\theta_{23} > 45°$), what is the value of CP violating phase δ, etc. Apart from these questions, the higher precision measurement of current neutrino mixing angles and mass square differences is also very

Table 1 Current best fit values of oscillation parameters and their 3 standard deviation range

Oscillation parameters	True values	Marginalisation range
$\sin^2(2\theta_{12})$	0.86	Fixed
$\sin^2(\theta_{23})$	0.5	0.4–0.6 (3σ range)
$\sin^2(\theta_{13})$	0.03	0.02–0.04 (3σ range)
Δm^2_{21} (eV^2)	7.6×10^{-5}	Fixed
Δm^2_{32} (eV^2)	2.4×10^{-3}	$(2.1$–$2.6) \times 10^{-3}$ (3σ range)
δ	0.0	Fixed

important. The current best fit values and errors in the oscillation parameters on the basis of global neutrino analyses [26–29] are summarised in Table 1. A large number of neutrino experiments are ongoing and proposed to achieve the above mentioned goals *viz.* MINOS [30], T2K [31], INO [32–34], PINGU [5], Hyper-Kamiokande [35], NOνA [36] etc. Present work is focused only on the magnetised Iron CALorimeter (ICAL) detector at the India-based Neutrino Observatory (INO).

India-based Neutrino Observatory (INO) is an approved project to construct an underground laboratory to be located at Theni district in southern India. The ICAL detector at INO will study mainly the atmospheric muon neutrinos and anti-neutrinos. Because of being magnetised, the ICAL detector can easily distinguish between atmospheric ν_μ and $\bar{\nu}_\mu$ by identifying the charge of muons produced in Charged-Current interactions of these neutrinos in the detector. Reconfirmation of atmospheric neutrino oscillations, precision measurement of oscillation parameters and the determination of neutrino mass hierarchy through the observation of earth matter effects in atmospheric neutrinos are the primary physics goals of the INO-ICAL experiment. Matter effects in neutrino oscillations are sensitive to the sign of Δm^2_{32}. Though the ICAL experiment is insensitive to δ [37], it has been observed that INO mass hierarchy results together with other experiments can help to determine the value of δ [38].

In this paper, we present the precision measurement of atmospheric neutrino oscillation parameters ($|\Delta m^2_{32}|$ and $\sin^2 \theta_{23}$) and θ_{23} deviation from the maximal mixing in a 3-flavor mixing scheme through the earth matter effect for the ICAL detector at INO.

The precision study of these parameters is important to assess the ICAL capability vis-a-vis other experiments. The sensitivity of the ICAL experiment for these oscillation parameters has already been studied by binning the events in the muon energy and muon angle, using realistic muon resolutions and efficiencies [39]. Here, however, we use a different approach to determine the sensitivity of the ICAL detector for the atmospheric neutrino mixing parameters. When an atmospheric $\nu_\mu (\bar{\nu}_\mu)$ interacts with the ICAL detector, it pro-

duces a $\mu^+ (\mu^-)$ and a shower of hadrons. In order to extract the full information about the parent neutrino, information of muons along with that of hadrons is used in the analysis. Recently, it has been shown that including hadron information together with the muon events improves the ICAL potential for the measurement of neutrino mass hierarchy [40,41]. Since the neutrino energy cannot be measured directly, therefore, in the analysis presented here, the neutrino energy is obtained by adding the energy deposited by the muons and hadron inside the ICAL detector. We then use this neutrino energy (E_ν) and muon angle ($\cos\theta_\mu$) as observables for the χ^2 estimation. An earlier analysis have used hadron information, but with constant resolutions to obtain the neutrino energy [42]. In the present work, we show the ICAL potential for the neutrino oscillation parameters using effective realistic ICAL detector resolutions.

The analysis starts with the generation of the neutrino events with NUANCE [43] and then events are binned into E_ν and $\cos\theta_\mu$ bins. Various resolutions and efficiencies obtained by the INO collaboration from a GEANT4 [44] based simulation are applied to these binned events in order to reconstruct the neutrino energy and muon direction. Finally, a marginalised χ^2 is estimated over the allowed ranges of neutrino parameters, other than θ_{23} and $|\Delta m^2_{32}|$, after including the systematic errors.

2 The ICAL detector and atmospheric neutrinos

The ICAL detector at INO [32,33] will be placed under approximately 1 km of rock cover from all directions to reduce the cosmic background. The detector will have three modules, each of size 16 m × 16 m × 14.45 m in the x, y and z directions respectively. ICAL consists of 151 horizontal layers of 5.6 cm iron plates with 4 cm of gap between two successive iron layers. Gaseous detectors called Resistive Plate Chambers (RPCs) of dimension 2 m × 2 m will be used as active detector elements and will be interleaved in the iron layer gap. RPC detectors are known for their good time resolution (∼1 ns) and spatial resolution (∼3 cm). The RPCs provide two dimensional readouts through the external copper pick up strips placed above and below the detector. Total mass of the detector is approximately 50 kt which will provide the statistically significant data to study the weakly interacting neutrinos. A magnetic field of upto 1.5 T will be generated through the solenoidal shaped coils placed around the detector [45,46]. The ICAL detector can easily identify the charge of muons due to this applied magnetic field, and hence, can easily distinguish between neutrinos and anti-neutrinos.

Atmospheric muon neutrinos and anti-neutrinos are the main sources of events for the ICAL detector. When cosmic rays interact with the earth's upper atmosphere, they produce pions which further decay into leptons and corresponding

neutrinos. The dominant channels of the decay chain producing atmospheric neutrinos, are

$$\pi^+ \to \mu^+ \nu_\mu, \quad \mu^+ \to e^+ \nu_e \bar{\nu}_\mu,$$
$$\pi^- \to \mu^- \bar{\nu}_\mu, \quad \mu^- \to e^- \bar{\nu}_e \nu_\mu. \tag{3}$$

Atmospheric neutrinos come in both ν_μ and ν_e ($\bar{\nu}_\mu$ and $\bar{\nu}_e$) flavors with the ν_μ flux almost double that of ν_e flux. Due to the large flight path and the wide coverage of the energy range (from few hundred MeV to TeV), atmospheric neutrinos play an important role in studying the neutrino oscillations. Neutrinos and anti-neutrinos interact differently with earth matter. We can use this special feature to measure the sign of Δm^2_{32}, and hence, the correct mass ordering.

3 Analysis

The atmospheric neutrino events are generated with the available 3-dimensional neutrino flux provided by HONDA et al. [47] using ICAL detector specifications. The interactions of atmospheric muon neutrino and anti-neutrino fluxes with the detector target are simulated by the NUANCE neutrino generator for 1000 years of exposure of the 50 kt ICAL detector. For the purpose of quoting the final sensitivity we normalise the 1000 years data to 10 years of exposure to keep Monte Carlo fluctuations under control; following a similar approach used in the earlier ICAL analyses [37,39]. The ICAL is highly sensitive to charged-current (CC) interactions where charged muons produced along with the hadron shower can be identified clearly though the RPC detectors. Since the resolutions and efficiencies studies for such events have been done by the INO collaboration [46,48] and are available, only the events generated through CC interactions are considered for the present analysis. It has been estimated that the background from the neutral current (NC) interactions for a magnetised iron neutrino detector (MIND), similar to ICAL, can be reduced to the level of about a percent, and the contribution of $\nu_\mu \to \nu_\tau$ oscillation background is between 1–4 % [49]. Therefore, we have neglected these effects in the current analysis for the time being.

Neutrino oscillations can be incorporated into the NUANCE code to generate the oscillated neutrino flux at the detector for different values of the oscillation parameters. However, this process requires large computational time and resources. Therefore, we simulate the interactions of atmospheric neutrinos with the detector in the absence of oscillations and the effect of oscillations is included by using the re-weighting algorithm described in Refs. [37,39]. For each neutrino event of a given energy E_ν and zenith direction θ_z, oscillation probabilities are estimated taking earth matter effects into account. The path length traversed by neutrinos from the production point to the detector, which is needed as

an input parameter in the oscillation probability estimation, is obtained as:

$$L = \sqrt{(R_{earth} + R_{atm})^2 - (R_{earth} \sin \theta_z)^2} - R_{earth} \cos \theta_z, \tag{4}$$

where R_{earth} is the radius of the earth and R_{atm} is the average height of the production point of neutrinos in the atmosphere. We have used $R_{earth} \approx 6371$ km and $R_{atm} \approx 15$ km. Here, we assume that $\cos \theta_z = 1$ is the downward and $\cos \theta_z = -1$ is the upward direction for incoming neutrinos. The oscillation parameters used in the analysis are listed in Table 1. For the precision measurement studies, we assume normal hierarchy of neutrinos.

In order to separate the muon neutrino and anti-neutrino events on the basis of their oscillation probabilities, each NUANCE generated unoscillated neutrino event was subjected to the oscillation randomly by applying the event re-weighting algorithm. Since ν_e may also change flavor to ν_μ due to oscillations, therefore, in order to include this contribution, we simulate the interactions of ν_e flux with the ICAL detector in the absence of oscillations using NUANCE and applying a re-weighting algorithm for the $\nu_e \to \nu_\mu$ channel. Hence, the total event spectrum consists of ν_μ events coming from both the oscillation channels (i.e. $\nu_\mu \to \nu_\mu$ and $\nu_e \to \nu_\mu$).

3.1 ICAL detector resolutions and the neutrino energy reconstruction

Due to the charged-current interaction of the neutrinos in the detector, muons along with the showers of hadrons are produced. Reconstruction of the neutrino energy requires the reconstruction of muon as well as hadron energy. Once we have the reconstructed muon and hadron energies, we directly add them together to get the final reconstructed neutrino energy. Muon and hadron energy resolutions have been obtained by the INO collaboration as a function of true energies and true directions of muons or hadrons using a GEANT4 [44] based code [39,46]. Muons give a clear track of hits inside the magnetised detector, therefore the energy of muons can be reconstructed easily using a track fitting algorithm. It was observed that the muons energy reconstructed by the ICAL detector follows a Gaussian distribution for $E_\mu \geq 1$ GeV whereas it follows a Landau distribution for $E_\mu < 1$ GeV. On the other hand, hadrons do not travel too far in the ICAL and hence they feel a negligible effect of the magnetic field before depositing their energies in a shower like pattern [48]. The total energy deposited by the hadron shower ($E'_{had} = E_\nu - E_\mu$) has been used to calibrate the detector response. It has been found that hadron hit patterns follow a Vavilov distribution [50]. The hadron energy resolution has been fitted as a function of E'_{had} [48]. In the present analy-
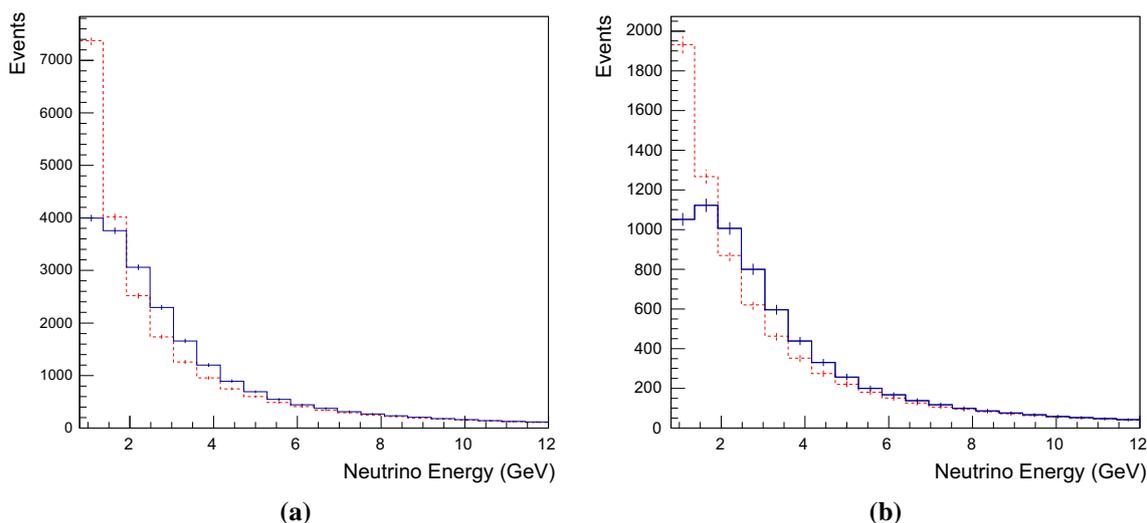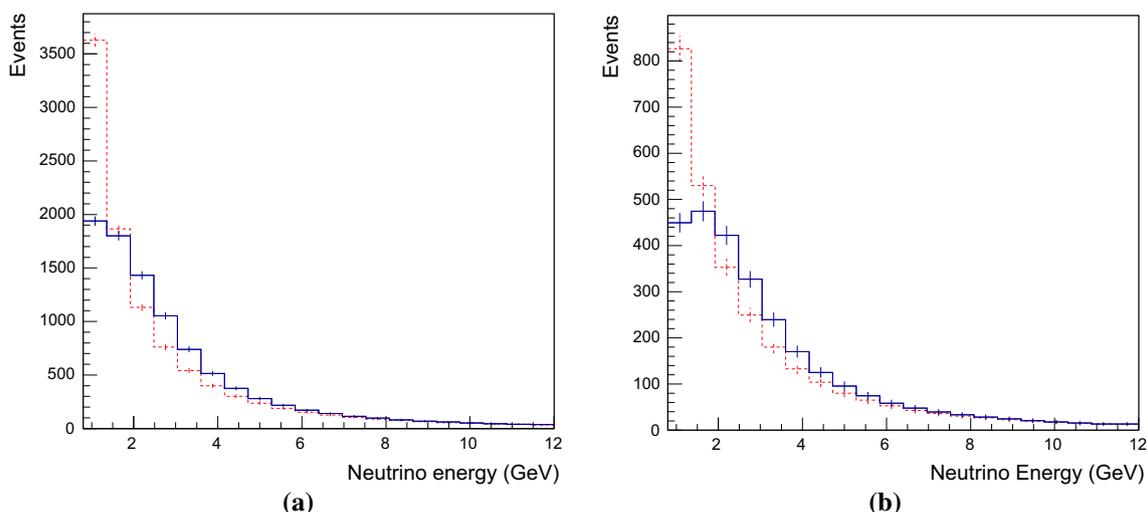
Fig. 1 True neutrino energy (*red-dashed line*) and the reconstructed neutrino energy (*blue-solid line*) from NUANCE simulated data for **a** neutrino events and **b** anti-neutrino events, from $\nu_\mu \to \nu_\mu$ oscillation channel

Fig. 2 True neutrino energy (*red-dashed line*) and the reconstructed neutrino energy (*blue-solid line*) from NUANCE simulated data for **a** neutrino events and **b** anti-neutrino events, from $\nu_e \to \nu_\mu$ oscillation channel

sis, muon energy and angular resolutions are implemented by smearing the true muon energy and direction of each μ^+ and μ^- event using the ICAL muon resolution functions [46]. True hadron Energies are smeared using the ICAL hadron resolution functions [48]. Reconstructed neutrino energy is then taken as the sum of smeared muon and hadron energy. Figure 1 shows the true and reconstructed neutrino and anti-neutrino energies obtained from the $\nu_\mu \to \nu_\mu$ channel while Fig. 2 shows the same for $\nu_e \to \nu_\mu$ channel. It can be seen that at lower incoming neutrino energies ($E_\nu \leq 1$), reconstruction of neutrino energy at ICAL is poor due to the effect of detector resolutions in this range.

Since the muon direction reconstruction is extremely good for ICAL, and hadron direction information not available yet,

we have used the reconstructed muon directions in the final analysis.

The reconstruction and charge identification efficiencies (CID) for μ^- and μ^+ for the ICAL detector are included into analysis by simply weighting each event with its reconstruction and relative charge identification efficiency. Though the CID efficiencies of the ICAL detector are $\geq 90\,\%$ beyond $E_\nu \sim 1$ GeV [46], it is still possible that some muon events (say μ^+) are wrongly identified as of the opposite charge particle (say μ^-). So, the total number of events reconstructed as μ^- will increase by

$$N^{\mu^-} = N_{RC}^{\mu^-} + (N_R^{\mu^+} - N_{RC}^{\mu^+}), \tag{5}$$

where N^{μ^-} are the number of total reconstructed μ^- events. $N_{RC}^{\mu^-}$ are the number of μ^- events reconstructed and correctly identified in charge and $N_{RC}^{\mu^+}$ are the number of μ^+ events with their respective reconstruction and CID efficiencies folded in; whereas $N_R^{\mu^+}$ are the number of μ^+ events with the reconstruction efficiency only. Hence, $N_R - N_{RC}$ gives the fraction of reconstructed events that have their charge wrongly identified. Total reconstructed μ^+ events can be obtained using a similar expression with charge reversal.

4 χ^2- Estimation

The sensitivity of the atmospheric neutrino oscillation parameters for ICAL is estimated by minimising the χ^2 for the neutrino data simulated for the ICAL detector. The re-weighted events, with detector resolutions and efficiencies folded in, are binned into reconstructed neutrino energy and muon direction for the determination of χ^2. The data has been divided into total 20 varied neutrino energy bins in the range of 0.8–10.8 GeV. Since most of the atmospheric neutrino events come below the neutrino energy $E_\nu \sim 5$ GeV, we have a finer energy binning with a bin width of 0.33 GeV from 0.8 to 5.8 GeV with a total of 15 energy bins. The high energy events, i.e. from 5.8 to 10.8 GeV, are divided into total 5 equal energy bins with a bin width of 1 GeV. A total of 20 $\cos\theta_\mu$ direction bins in the range $[-1, 1]$ with equal bin width, have been chosen. The bin size for the analysis has been optimised such that each bin contains at least one event. The above mentioned binning scheme is applied for both ν_μ and $\bar{\nu}_\mu$ events.

We use the maximal mixing, that is, $\sin^2\theta_{23} = 0.5$ as the reference value. The atmospheric mass square splitting is related to the other oscillation parameters, so for the precision study we have used Δm_{eff}^2, which can be written as [37,51],

$$\Delta m_{eff}^2 = \Delta m_{32}^2 \\ -(\cos^2\theta_{12} - \cos\delta\sin\theta_{23}\sin2\theta_{12}\tan\theta_{23})\Delta m_{21}^2. \tag{6}$$

The other oscillation parameters (θ_{12}, Δm_{21}^2 and δ) are kept fixed both for observed and predicted events as the marginalisation over these parameters has negligible effects on the analysis results. Since in our analysis, the event samples are distributed in terms of reconstructed neutrino energy and the muon zenith angle bins, we call these events as neutrino-like events that is, we refer to N^{μ^-} as $N(\nu_\mu)$ and N^{μ^+} as $N(\bar{\nu}_\mu)$.

The various systematic effects on the χ^2 have been implemented through five systematic uncertainties, *viz.* 20 % error on atmospheric neutrino flux normalisation, 10 % error on neutrino cross-section, a 5 % uncertainty due to zenith angle dependence of the fluxes, an energy dependent tilt error, and

an overall 5 % statistical error, as applied in earlier ICAL analyses [37,39]. The systematic uncertainties are applied using the method of "pulls" as outlined in Ref. [52]. Briefly, in the method of pulls, systematic uncertainties and the theoretical errors are parameterised in terms of set of variables ζ_k, called pulls. Due to the fine binning, some bins may have very small number of entries, therefore, we have used the poissonian definition of χ^2 given as

$$\chi^2(\nu_\mu) = min \sum_{i,j} \Bigg(2(N_{ij}^{th'}(\nu_\mu) - N_{i,j}^{ex}(\nu_\mu)) \\ + 2N_{i,j}^{ex}(\nu_\mu)(\ln\frac{N_{i,j}^{ex}(\nu_\mu)}{N_{i,j}^{th'}(\nu_\mu)}) \Bigg) + \sum_k \zeta_k^2, \tag{7}$$

where

$$N_{ij}^{th'}(\nu_\mu) = N_{i,j}^{th}(\nu_\mu)\left(1 + \sum_k \pi_{ij}^k \zeta_k\right). \tag{8}$$

Here, N_{ij}^{ex} are the observed number of reconstructed μ^- events, as calculated from Eq. (5), generated using true values of the oscillation parameters as listed in Table 1 in the ith neutrino energy bin and jth $\cos\theta_\mu$ bin. In Eq. (8), N_{ij}^{th} are the number of theoretically predicted events generated by varying oscillation parameters, $N_{ij}^{th'}$ represents the modified events spectrum due to the systematic uncertainties, π_{ij}^k is the systematic shift in the events of ith neutrino energy bin and jth $\cos\theta_\mu$ bin due to kth systematic error. ζ_k is the univariate pull variable corresponding to the π_{ij}^k uncertainty. An expression similar to Eq. (7) can be obtained for $\chi^2(\bar{\nu}_\mu)$ using reconstructed μ^+ event samples. We have calculated $\chi^2(\nu_\mu)$ and $\chi^2(\bar{\nu}_\mu)$ separately and then these two are added to get total χ_{total}^2 as

$$\chi_{total}^2 = \chi^2(\nu_\mu) + \chi^2(\bar{\nu}_\mu). \tag{9}$$

We impose the recent θ_{13} measurement as a prior while marginalising over $\sin^2\theta_{13}$ as

$$\chi_{ical}^2 = \chi_{total}^2 + \left(\frac{\sin^2\theta_{13}(true) - \sin^2\theta_{13}}{\sigma_{\sin^2\theta_{13}}}\right)^2. \tag{10}$$

The value of $\sigma_{\sin^2\theta_{13}}$ was taken as 10 % of the true value of $\sin^2\theta_{13}$.

Finally, in order to obtain the experimental sensitivity for θ_{23} and $|\Delta m_{32}^2|$, we minimise the χ_{ical}^2 function by varying oscillation parameters within their allowed ranges over all systematic uncertainties.

The octant sensitivity for ICAL has been estimated using neutrino-like events considering Normal hierarchy. The significance of ruling out the wrong octant is given by

$$\Delta\chi^2 = \chi^2(false\ octant) - \chi^2(true\ octant), \tag{11}$$

where χ^2 (true octant) has been obtained by considering both the predicted and observed event spectrum in the true octant while the χ^2 (false octant) has been obtained by assuming predicted events with the true octant and observed events with the false octant. Note that for this study we kept all the oscillation parameters fixed and the analysis has been performed for different true values of $\sin^2 \theta_{23}$.

We also performed the mass hierarchy determination using analysis method and the oscillation parameters discussed in this paper and found no appreciable improvement in the hierarchy determination over muon angle and muon energy analysis [37] as already verified earlier [40].

5 Results

The two dimensional confidence region of the oscillation parameters ($|\Delta m_{eff}^2|$, $\sin^2 \theta_{23}$) are determined from $\Delta \chi_{ical}^2$ around the best fit. The resulting region is shown in Fig. 3. These contour plots have been obtained assuming $\Delta \chi_{ical}^2 = \chi_{min}^2 + m$, where χ_{min}^2 is the minimum value of χ_{ical}^2 for each set of oscillation parameters and values of m are taken as 2.30, 4.61 and 9.21 corresponding to 68, 90 and 99 % confidence levels [23] respectively for two degrees of freedom. Figure 4a depicts the one dimensional plot for the measurement of test parameter $\sin^2 \theta_{23}$ at constant value of $|\Delta m_{eff}^2| = 2.4 \times 10^{-3}$ (eV^2) and Fig. 4b for the $|\Delta m_{eff}^2|$ at constant $\sin^2 \theta_{23} = 0.5$ at 1σ, 2σ and 3σ levels for one parameter estimation [23].

The precision on the oscillation parameters can be defined as:

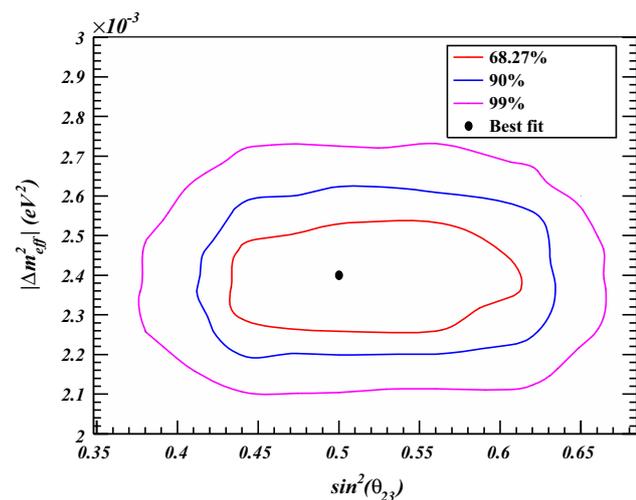$$Precision = \frac{P_{max} - P_{min}}{P_{max} + P_{min}}, \tag{12}$$

(a)

(b)

Fig. 4 **a** $\Delta \chi^2$ as a function of different test values of $\sin^2 \theta_{23}$ and **b** $\Delta \chi^2$ as a function of different input values of $|\Delta m_{32}^2|$

where P_{max} and P_{min} are the maximum and minimum values of the oscillation parameters concerned at a given confidence level. The current study shows that ICAL is capable of measuring the atmospheric mixing angle $\sin^2 \theta_{23}$ with a precision of 13, 21 and 27 %, at 1σ, 2σ and 3σ confidence levels respectively. The atmospheric mass square splitting $|\Delta m_{32}^2|$ can be measured with a precision of 4, 8 and 12 % at 1 σ, 2 σ and 3 σ confidence levels respectively. These numbers show an improvement of 20 and 23 % on the precision measurement of $\sin^2 \theta_{23}$ and $|\Delta m_{32}^2|$ parameters respectively at 1σ level over muon energy and muon direction analysis [39]. These results shows that the inclusion of hadron information together with muon information significantly improves the capability of the ICAL detector for the estimation of oscillation parameters. These results may further be improved by including the neutrino direction in the χ^2 definition, a work under progress in the INO collaboration.

Fig. 3 Contour plots for $\sin^2 (\theta_{23})$ and $|\Delta m_{eff}^2|$ measurements at 68, 90 and 99 % confidence level for 10 years exposure of ICAL detector
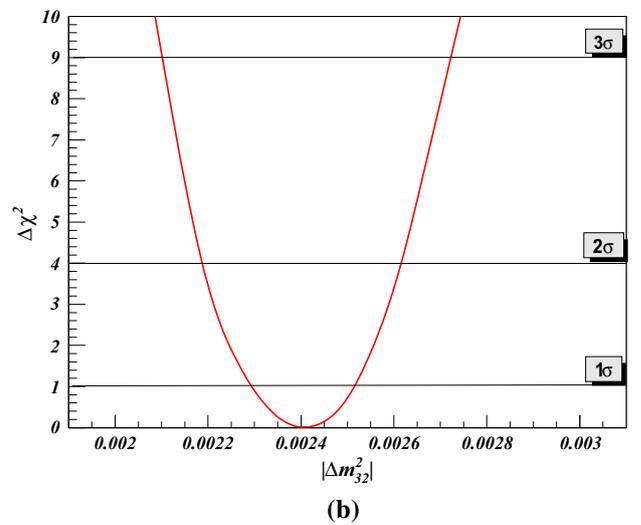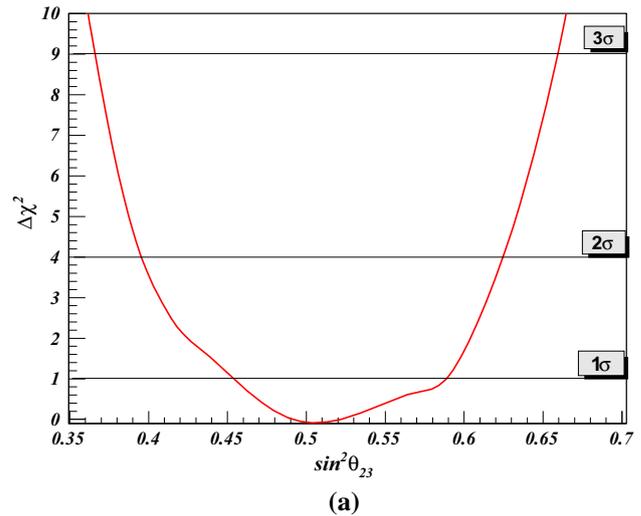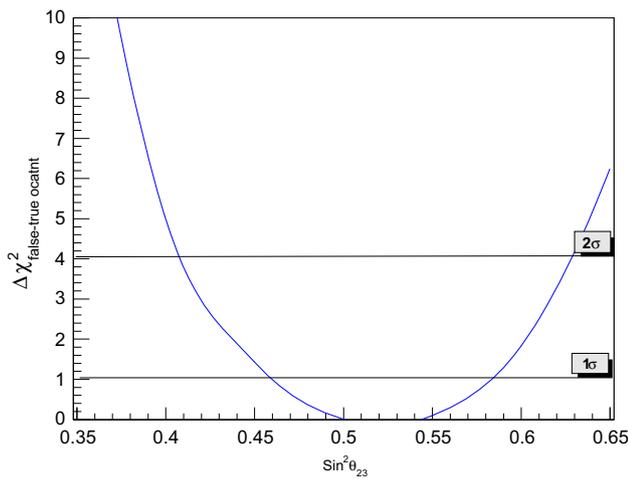
Fig. 5 $\Delta\chi^2_{false-true\ octant}$ for different input values of $\sin^2\theta_{23}$

Figure 5 show the χ^2 plot for the identification of octant sensitivity for different true values of $\sin^2\theta_{23}$ assuming Normal hierarchy. It can be seen from this figure that using neutrino energy and muon direction as two dimensional observables, ICAL can identify the lower octant when $\sin^2\theta_{23} < 0.46$ ($\sin^2\theta_{23} < 0.40$) with 1σ (2σ) confidence levels. Similarly, the higher octant can be identified when $\sin^2\theta_{23} > 0.58$ ($\sin^2\theta_{23} > 0.63$) with 1σ (2σ) confidence levels. It has also been observed that the ICAL sensitivity deteriorates on approaching the θ_{23} closer to its maximal mixing value ($\sin^2\theta_{23} = 0.5$).

The two-dimensional contour plots in the $\sin^2\theta_{23}$ and Δm^2_{32} plane provides the significance levels for the octant sensitivity assuming the true lower octant value ($\sin^2\theta_{23} = 0.4$) and true higher octant value ($\sin^2\theta_{23} = 0.65$) and is shown in Fig. 6. It can be seen from Fig. 6 that the ICAL

is able to determine the deviation of θ_{23} from the maximal mixing upto 2σ confidence level in 10 years of running. The results presented here for octant sensitivity studies are comparable with the results of the three-dimensional analysis using hadron information at ICAL [41].

6 Conclusions

The magnetised ICAL detector at INO has a potential to reveal several neutrino properties, especially the mass hierarchy of the neutrino through earth matter effect and a comprehensive information on neutrino oscillation parameters. We have studied the ICAL detector capability for the precise measurement of atmospheric neutrino oscillation parameters using neutrino energy and muon angle as observables. A Monte Carlo simulation using NUANCE generated neutrino data for 10 years exposure of the ICAL detector has been carried out. The analysis has been performed in the framework of three neutrino flavor mixing and by taking the earth matter effect into account. A marginalised χ^2 analysis in fine bins of reconstructed neutrino energy and muon angle has been performed. Realistic detector resolutions and efficiencies, generated from ICAL detector simulation have been utilised. The effect of various systematic uncertainties have also been included in the analysis.

The current analysis takes into account ν_μ events coming from CC interactions. However, there will also be a small ($\sim 1\%$) contribution from NC interactions and from the ν_τ CC interactions which we have neglected for the time being. These small effects are being studied and will be included in the future ICAL analysis. Moreover, this study is a demonstration of the fact that the ICAL experiment has the capabil-
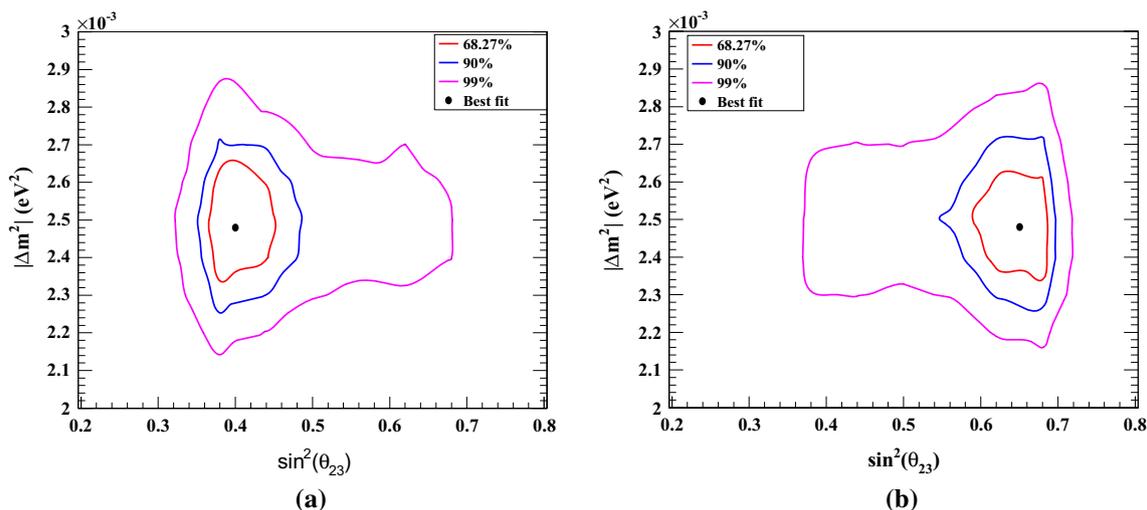

Fig. 6 Contour plots indicating 68, 90 and 99 % CL **a** at true $\sin^2\theta_{23} = 0.4$ and **b** at true $\sin^2\theta_{23} = 0.65$ assuming NH is true for 10 year of ICAL exposure. The fluctuations in the plots results from the implementation of resolutions and efficiencies through Monte-Carlo method

ity of harnessing hadron information to further improve the measurement of oscillation parameters.

We conclude that by using reconstructed neutrino energy and muon direction there is an average improvement of about 20 % on the precision measurement of both the parameters ($\sin^2 \theta_{23}$ and $|\Delta m_{32}^2|$) over muon energy, muon angle analysis [39]. The octant sensitivity study shows that ICAL is able to discrimante the octant of θ_{23} with a significance of 2σ for 10 year exposure. The mass hierarchy determination using the present analysis does not improve significantly over the muon energy and muon angle only analysis.

References

1. Y. Fukuda et al., Phys. Rev. Lett. **81**(8), 1562–1567 (1998). arXiv:hep-ex/9807003
2. R. Wendell et al., Super-Kamiokande Collaboration, Phys. Rev. D **81**, 092004 (2010)
3. P. Adamson et al., MINOS Collaboration, Phys. Lett. **110**, 251801 (2013)
4. K. Abe et al., T2K Collaboration, Phys. Rev. Lett. **112**, 181801 (2014)
5. D.J. Koskinen, Mod. Phys. Lett. A **26**, 2899 (2011)
6. B.T. Cleveland et al., Astrophys. J. **496**, 505 (1998)
7. F. Kaether, W. Hampel, G. Heusser, J. Kiko, T. Kirsten, Phys. Lett. B **685**, 47 (2010)
8. J.N. Abdurashitov et al., SAGE Collaboration, Phys. Rev. C **80**, 015807 (2009)
9. G. Bellini, J. Benziger, D. Bick, S. Bonetti, G. Bonfini et al., Phys. Rev. Lett. **107**, 141302 (2011)
10. B. Aharmim et al., SNO. Phys. Rev. Lett. **101**, 111301 (2008)
11. B. Aharmim et al., SNO. Phys. Rev. C **81**, 055504 (2010)
12. J. Hosaka et al., (Super-Kamkiokande Collaboration), Phys. Rev. D **73**, 112001 (2006). arXiv:hep-ex/0508053
13. J. Cravens et al., Super-Kamiokande Collaboration, Phys. Rev. D **78**, 032002 (2008)
14. K. Abe et al., Super-Kamiokande Collaboration, Phys. Rev. D **83**, 052010 (2011)
15. A. Renshaw, (Super-Kamiokande Collaboration), (2014). arXiv:1403.4575v1
16. A. Renshaw et al. (Super-Kamiokande Collaboration), Phys. Rev. Lett. **112**, 091805 (2014). arXiv:1312.5176
17. S. Abe et al., (KamLAND Collaboration), Phys. Rev. Lett. **100**, 221803 (2008). arXiv:0801.4589
18. Y. Abe et al., Double Chooz Collaboration, Phys. Rev. D **86**, 052008 (2012)
19. F. An et al. (DAYA-BAY Collaboration), Phys. Rev. Lett. **108**, 171803 (2012). arXiv:1203.1669
20. J. Ahn et al., (RENO collaboration), Phys. Rev. Lett. **108**, 191802 (2012). arXiv:1204.0626
21. B. Pontecorvo, Sov. Phys. JETP **26**, 984 (1968). [Zh. Eksp. Teor. Fiz **53**, 1717 (1967)]
22. Z. Maki, M. Nakagawa, S. Sakata, Prog. Theor. Phys. **28**, 870 (1962)
23. K. Nakamura et al., J. Phys. G: Nucl. Part. Phys. **37**, 075021 (2010)
24. P. Adamson et al., Phys. Rev. Lett. **110**, 171801 (2013)
25. K. Abe et al., T2K Collaboration, Phys. Rev. Lett. **112**, 061802 (2014)
26. G.L. Folgi et al. (2012). arXiv:1205.5254] [hep-ph]
27. M.C. Gonzalez-Gracia et al., JHEP **1212**, 123 (2012). arXiv:1209.3023 [hep-ph]
28. F. Capozzi et al., Phys. Rev. D **89**, 093018 (2013). arXiv:1312.2878
29. M.C. Gonzalez-Gracia, *Physics of the Dark Universe*, pp. 41–5 (2014)
30. For instance see http://www-numi.fnal.gov/PublicInfo/forscientists.html
31. T2K report (2013). http://www.t2k.org/docs/pub/015
32. S. Atthar et al., (INO Collaboration), The Technical Design Report of INO-ICAL Detector (2006)
33. India-based Neutrino Observatory (INO). http://www.ino.tifr.res.in/ino/
34. D. Kaur et al., Nucl. Instrum. Methods Phys Res Sect A **774**, 74–81 (2015)
35. K. Abe et al. (2011). arXiv:1109.3262 [hep-ex]
36. D.S. Ayres et al., NOνA Collaboration. arXiv:hep-ex/0503053 [hep-ex]
37. A. Ghosh et al., JHEP **04**, 009 (2013)
38. M. Ghosh et al., Phys. Rev. D **89**, 011301 (2014). arXiv:1306.2500
39. T. Thakore et al., JHEP **05**, 058 (2013)
40. A. Ghosh, S. Choubey, JHEP **2013**, 174 (2013). arXiv:1306.1423v1 [hep-ph]
41. M.M. Devi et al., JHEP **10**, 189 (2014). arXiv:1406.3689v1 [hep-ph]
42. A. Samanta et al., JHEP **1107**, 048 (2011). arXiv:1012.0360 [hep-ph]
43. D. Casper, Nucl. Phys. Proc. Suppl. **112**, 161 (2002). arXiv:hep-ph/0208030
44. GEANT Simulation Toolkit. http://wwwasd.web.cern.ch/wwwasd/geant/
45. S.P. Behera et al. (2014). arXiv:1406.3965 [physics.ins-det]
46. A. Chatterjee et al., JINST **9**, P007001 (2014). arXiv:1405.7243v1 [physics.ins-det]
47. M. Honda, T. Kajita, K. Kasahara, S. Midorikawa, Phys. Rev. D **70**, 043008 (2004). arXiv:astro-ph/0404457
48. M.M. Devi et al., JINST **8**, P11003 (2013)
49. R. Bayes et al., Phys. Rev. D **86**, 093015 (2012). arXiv:1208.2735
50. A. Rotondi, P. Montagna, Nuclear Instrum. Methods B **47**, 215–223 (1990)
51. H. Nunokawa, S.J. Parke, R. Zukanovich Funchal, Phys. Rev. D **72**, 013009 (2005). arXiv:hep-ph/0503283
52. M.C. Gonzalez-Garcia, M. Maltoni et al., Phys. Rev. D **70**, 033010 (2004). arXiv:hep-ph/0404085v1